

Some gross features of non-central heavy ion collisions

First results of the INDRA@GSI Campaign

J. Łukasik^{6,10}, A.S. Botvina⁶, G. Auger¹, Ch.O. Bacri², M.L. Begemann-Blaich⁶, N. Bellaïze³, R. Bittiger⁶, F. Bocage³, B. Borderie², R. Bougault³, B. Bouriquet¹, Ph. Buchet⁴, J.L. Charvet⁴, A. Chbihi¹, R. Dayras⁴, D. Doré⁴, D. Durand³, J.D. Frankland¹, E. Galichet⁵, D. Gourio⁶, D. Guinet⁵, S. Hudan¹, B. Hurst³, H. Orth⁶, P. Lantusse⁵, F. Lavaud², J.L. Laville¹, C. Leduc⁵, A. Le Fevre⁶, R. Legrain⁴, O. Lopez³, U. Lynen⁶, W.F.J. Müller⁶, L. Nalpas⁴, E. Plagnol², E. Rosato⁷, A. Saija⁸, C. Sfienti⁶, C. Schwarz⁶, J.C. Steckmeyer³, G. Tăbăcaru¹, B. Tamain³, W. Trautmann⁶, A. Trzciński⁹, K. Turzó⁶, E. Vient³, M. Vigilante⁷, C. Volant⁴ and B. Zwiegliński⁹.
(The INDRA and the ALADIN Collaboration)

¹ GANIL, CEA et IN2P3-CNRS, B.P. 5027, F-14076 Caen, France.

² Institut de Physique Nucléaire, IN2P3-CNRS et Université, F-91406 Orsay, France.

³ LPC, IN2P3-CNRS, ISMRA et Université, F-14050 Caen, France.

⁴ DAPNIA/SPhN, CEA/Saclay, F-91191 Gif sur Yvette, France.

⁵ Institut de Physique Nucléaire, IN2P3-CNRS et Université, F-69622 Villeurbanne, France.

⁶ Gesellschaft für Schwerionenforschung mbH, D-64291 Darmstadt, Germany.

⁷ Dipartimento di Scienze Fisiche e Sezione INFN, Univ. Federico II, I-80126 Napoli, Italy.

⁸ Dipartimento di Fisica dell' Università and INFN I-95129 Catania, Italy.

⁹ Soltan Institute for Nuclear Studies, PL-00681 Warsaw, Poland.

¹⁰ H. Niewodniczański Institute of Nuclear Physics, PL-31342 Kraków, Poland.

Abstract

Experimental data obtained with the 4π multi-detector system INDRA set up on the beam delivered by SIS, were used to study peripheral and semi-central collisions of Au and Au at energies between 40 and 150 MeV/nucleon.

The analysis was performed as a function of incident energy and of impact parameter, defined through the total transverse energy of light charged particles (Etrans12). This observable was found to be a suitable measure of centrality of the collision for both symmetric and asymmetric systems. For a given system, Etrans12 was found to scale linearly with the available energy. Deviations from linear scaling above certain limits of the available energy are discussed.

Strong forward-backward asymmetries in the emission pattern with respect to the rapidities of the projectile and target residues are observed. Their possible relation to equilibration is discussed and interpreted in the framework of statistical multifragmentation and molecular dynamics models.

Transverse momenta of intermediate mass fragments produced in the midrapidity region are analyzed. The spectra are found to show little dependence on impact parameter implying some scenarios of their origin.

1 Introduction

High quality experimental data obtained with the 4π multi-detector system INDRA set up on the beam delivered by SIS offer a unique opportunity to perform a detailed study, including the isospin degree of freedom, of the collisions of both symmetric (Au+Au, Xe+Sn) and asymmetric (C+Au, C+Sn) systems in a broad energy range. It covers an interesting transition region from around the Fermi energy (40-50 MeV/nucleon) up to relativistic

energies approaching the participant-spectator domain (150-250 MeV/nucleon) for symmetric systems, and a range of relativistic bombarding energies (95-1800 MeV/nucleon) for asymmetric ones.

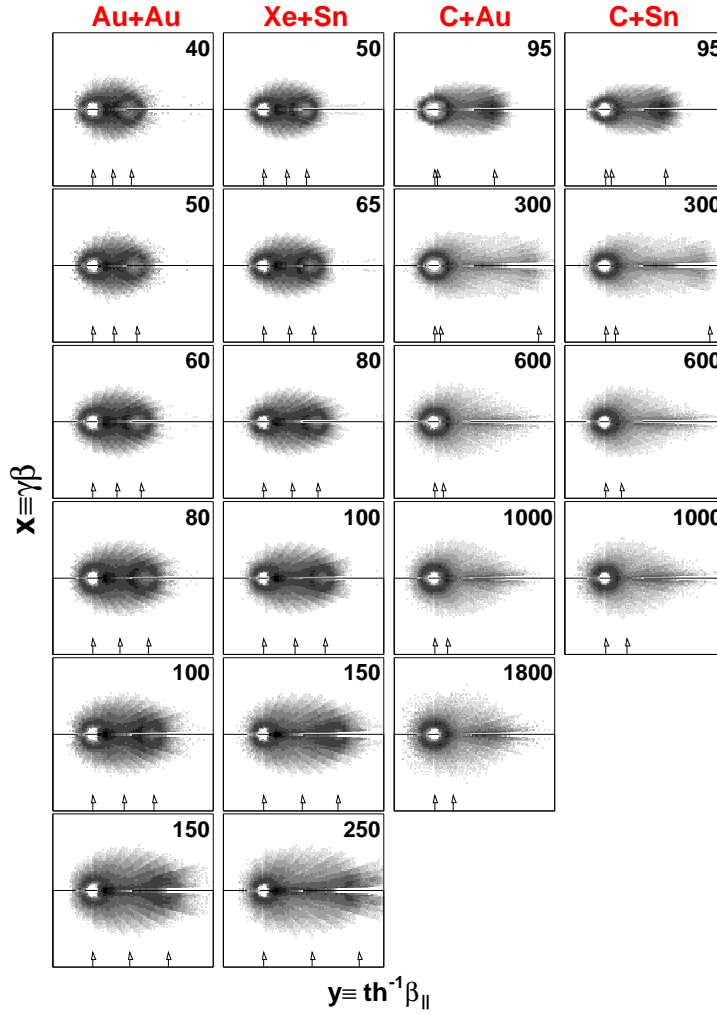


Figure 1: Invariant cross sections of helium ions measured for peripheral collisions of Au+Au, Xe+Sn C+Au and C+Sn at various energies per nucleon of the projectile indicated in the right top corners of the panels. The spectra were taken for the second most peripheral bin out of 8 impact parameter bins defined through the total transverse energy of light charged particles (Etrans12, see sect. 2 for more details). The arrows denote, from the left to the right, the target, CM and projectile rapidities, respectively.

Non-central collisions of symmetric heavy systems turn out to be essentially of binary character with pronounced projectile and target like sources (see left part of Fig. 1). Collisions of asymmetric systems, in turn, (see right part of Fig. 1) lead to a main single source picture with asymmetric emission patterns in velocity space.

Despite of the pronounced binary character of symmetric heavy ion collisions, a sizable amount of detected particles and fragments have parallel velocities intermediate between those of the projectile and of the target [1] - [3] and their importance increases with the increasing centrality of the collision. They are often referred to as midrapidity (-velocity) emissions.

These emissions seem to be strongly influenced by dynamical effects and are thought to proceed on a relatively short time scale. One can imagine various scenarios of formation of those midrapidity fragments following the predictions of various dynamical or hydrodynamical models. These scenarios include fast pre-equilibrium particles, neck emitted particles and fragments, as well as light fission fragments preferentially aligned in between the two main reaction partners.

Numerous analyses assume the existence of a well-characterized, thermal-like source. Can midrapidity emissions be regarded as originating from such a source? If yes, than to what extent? This is the main issue we would like to raise in this contribution.

2 Centrality selection

It is a well known fact, illustrated by dynamical calculations, that the reaction mechanism and the associated dissipation, spin, mass and charge transfer are very dependent on the impact parameter of the collision which, however, cannot be measured directly. Therefore an event selector, based on observed quantities, has to be defined and adapted to the detector setup. One of the properties of the INDRA detector [4] is its high efficiency (about 90%) for light charged particles (LCP, $Z=1,2$), independently of the type of the reaction mechanism involved and hence of the impact parameter. In the following we use the total laboratory transverse energy, $E_{\text{trans}12}$, of LCP as an impact parameter selector.

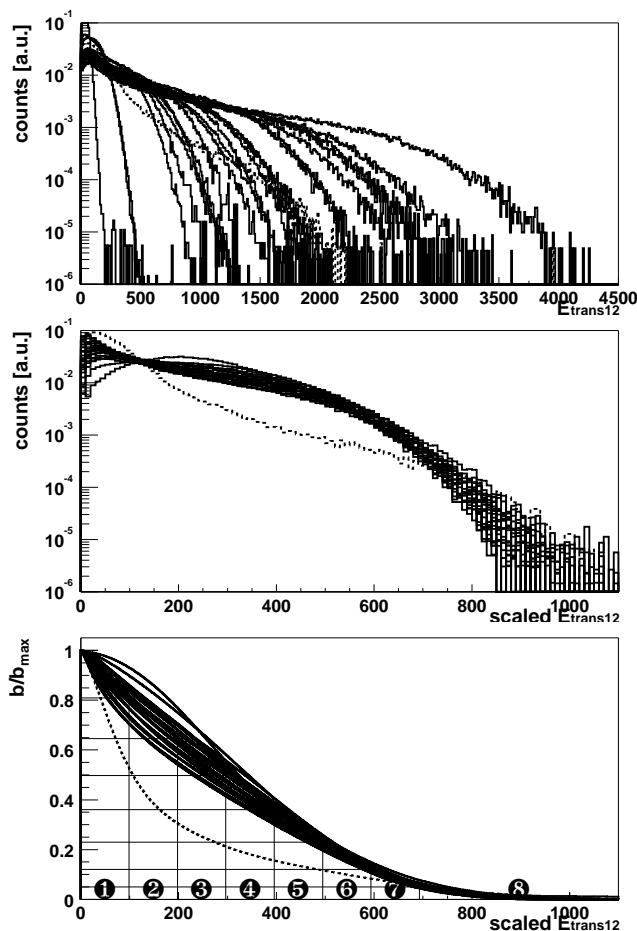


Figure 2: Upper panel: the spectra of the transverse energy of $Z=1$ and $Z=2$ particles ($E_{\text{trans}12}$) for 23 main systems studied during the 4th INDRA Campaign: Au+Au @ 40, 50, 60, 80, 100, 150, Xe+Sn @ 50, 65, 80, 100, 150, 250, C+Au @ 30, 95, 300, 600, 1000, 1800, C+Sn @ 95, 300, 600, 1000 MeV/nucleon (solid lines) and C+U @ 1000 MeV/nucleon (dashed line); middle panel: the same spectra but scaled to that for Xe+Sn @ 50 MeV/nucleon; bottom panel: reduced impact parameter derived from the scaled spectra with the indicated binning of $E_{\text{trans}12}$ and b/b_{max} for Au+Au @ 60 MeV/nucleon reaction. Note that the equal binning in $E_{\text{trans}12}$ results in nonequal binning of b/b_{max} which is still system/energy dependent.

The upper panel of Fig. 2 presents distributions of this observable for the 23 main systems studied during the 4th INDRA Campaign: Au+Au @ 40, 50, 60, 80, 100, 150,

Xe+Sn @ 50, 65, 80, 100, 150, 250, C+Au @ 30, 95, 300, 600, 1000, 1800, C+Sn @ 95, 300, 600, 1000 and C+U @ 1000 MeV/nucleon. The last reaction is indicated by a dashed line in all panels.

The middle panel presents an interesting scaling feature of Etrans12. As can be seen, all the spectra have similar shapes, and by changing the Etrans12 scale they can be superimposed on top of each other for both symmetric and asymmetric systems. The only exception seems to be the reaction C+U @ 1000 MeV/nucleon, probably indicating a different character of reactions with high fissility partners. The Etrans12 scale used for the abscissa is that of the Xe+Sn @ 50 MeV/nucleon system.

The bottom panel presents the relation between the Etrans12 and the reduced impact parameter, b/b_{max} , obtained with the use of the geometrical prescription [5]. The maximum impact parameter b_{max} is determined by the experimental trigger and thus refers to the events with at least 4 (symmetric systems) or 5 (asymmetric systems) charged particles or fragments detected. The last bin (8) corresponds to 5% of the maximum reduced impact parameter. The remaining part of the Etrans12 spectrum was divided into 7 equal bins, with bin 1 corresponding to the most peripheral collisions.

It seems also worthwhile to take a closer look at the scaling property of Etrans12. Fig. 3 presents the relation between the Etrans12 for the most central bin (8) and the available energy in the CM of the system for Au+Au, Xe+Sn, C+Au and C+Sn reactions. The first 4 points for the Xe+Sn reaction (25, 32, 39 and 45 MeV/nucleon) come from the 1st INDRA Campaign [3] conducted at GANIL.

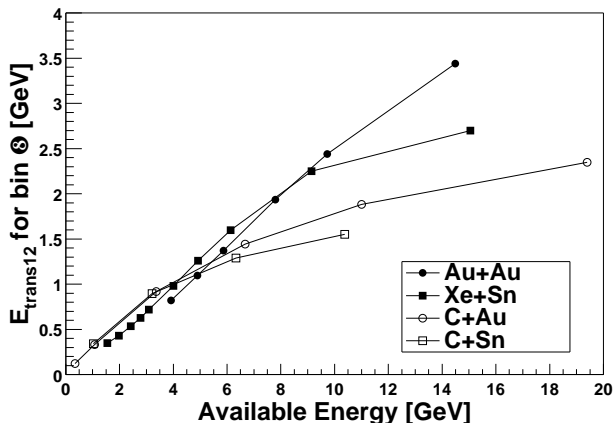


Figure 3: Etrans12 for the most central bin versus the available energy in the CM of the systems: Au+Au @ 40, 50, 60, 80, 100, 150, Xe+Sn @ 25, 32, 39, 45, 50, 65, 80, 100, 150, 250, C+Au @ 30, 95, 300, 600, 1000, 1800 and C+Sn @ 95, 300, 600, 1000 MeV/nucleon.

For symmetric systems, the scaling factor of the spectra from the middle panel of Fig. 2 is just the available energy in the CM system, up to about 100-150 MeV/nucleon (see also [3]). Above this threshold a saturation effect can be observed. For asymmetric systems the saturation is clearly visible above 300 MeV/nucleon. One can find at least 2 reasons for this saturation effect above a certain threshold energy. The first one is instrumental, namely, the number of multihits and punch-through hits increases with increasing incident energy leading to a higher level of mis- or nonidentification or imperfect energy calibration. The second, physical, effect is related to the fact that at relativistic energies the nucleon-nucleon cross section becomes more forward peaked reducing the conversion of incident energy into transverse energy and leading to some transparency effects. At high energies the particle production channels also start to be of importance.

3 Midrapidity emissions

As has already been shown in Fig. 1, the pronounced two source picture of peripheral symmetric heavy ion collisions was always (even at highest, 150 MeV/nucleon energy) accompanied by an important contribution of midrapidity heliums. How does this picture evolve with the mass of the emitted fragments?

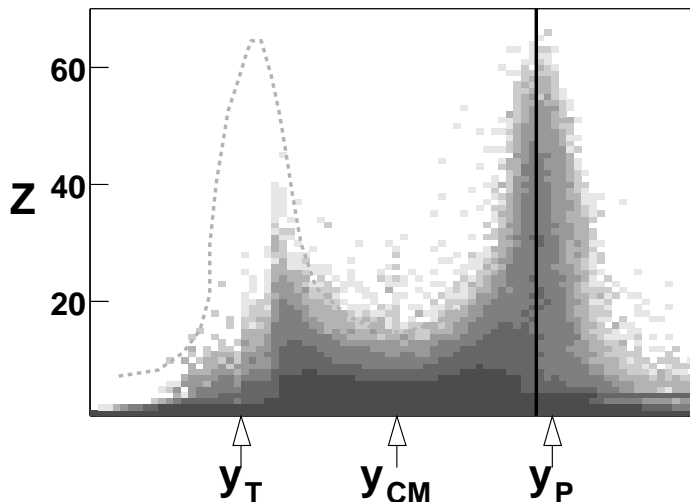


Figure 4: Contour plot of Z vs rapidity for fragments from peripheral collisions of Au+Au at 80 MeV/n. The dashed line marks the target-side region which is affected by detection thresholds. The arrows denote the target, CM and projectile rapidities, respectively.

Fig. 4 presents rapidity distributions of fragments emitted in the reaction Au+Au at 80 MeV/n at large impact parameters (bin 3). The vertical line corresponds to the mean rapidity of heavy projectile-like fragments. It is drawn to emphasize the strong forward-backward asymmetry in the emission of lighter fragments. The dashed line indicates the, expected from the symmetry of the system, target-side region which is affected by detection thresholds. The arrows denote the target, CM and projectile rapidities, respectively. The figure clearly shows that intermediate mass fragments (IMFs, $3 \leq Z \leq 20$) are preferentially emitted towards midrapidity, in between the rapidities of the heavy target and projectile residua.

3.1 Can they be thermal?

Certainly not all of them, but at least a fraction of these emissions, in the vicinity of the Coulomb rings (Fig. 1), can be interpreted in the framework of statistical multifragmentation models like SMM [6] or MMMC [7], provided that the Coulomb influence of the heavy partner on the (multi)fragmenting excited nucleus is taken into account. Inclusion of, preferentially elliptical, flow and angular momentum effects also seems to be important.

Fig. 5 presents SMM predictions for the invariant cross sections of lithium fragments emitted in peripheral collision of Au+Au @ 80 MeV/nucleon (insets) and three slices along the target, CM and projectile rapidities (upper row) and projections on rapidity axis (lower row). The gold sources were assumed to be excited up to 3 MeV/nucleon and to multifragment after 200 fm/c. The left column presents the results of the original SMM model, in the middle column, the effect of the Coulomb field of the heavy partner on the partitioning nucleus and a radial flow of 1.5 MeV/nucleon have been included, and in the right column an additional elliptical flow aligned along the beam direction was assumed instead of a radial one.

Au+Au @ 80 MeV/n | Z=3

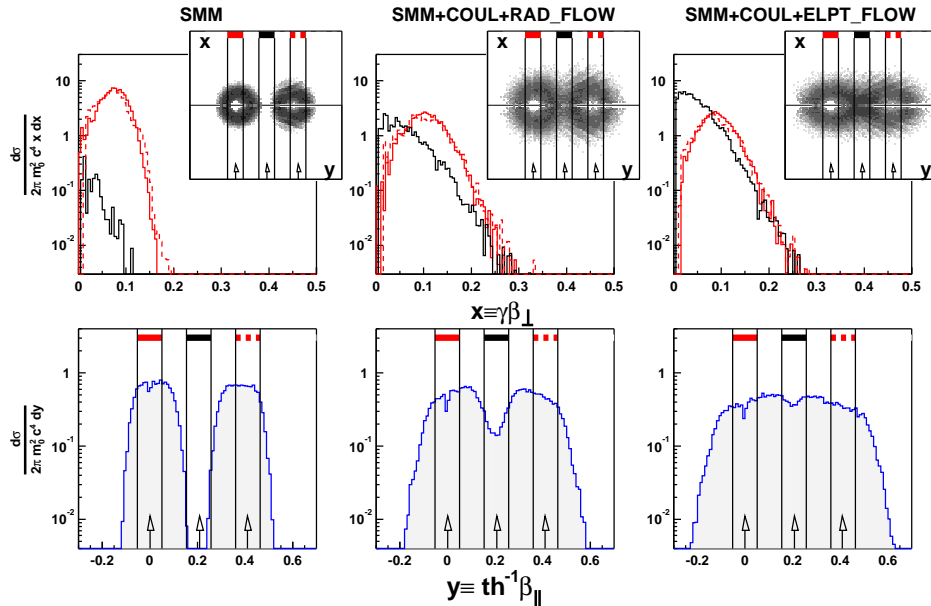


Figure 5: SMM predicted invariant cross sections of lithium fragments emitted in peripheral reaction of Au+Au @ 80 MeV/n (insets) and their slices along the target, CM and projectile rapidities (upper row) and projections on rapidity axis (lower row). The gold sources are assumed to be excited to 3 MeV/nucleon and multifragment after 200 fm/c. Left column: original SMM; middle column: SMM including the Coulomb field effect of the partner nucleus on the partitioning nucleus and a radial flow of 0.15 MeV/nucleon; right column: same as middle one but elliptical flow is assumed instead of a radial one.

As can be seen, the original SMM model, without the mutual Coulomb influence, predicts the emission patterns symmetric about the source rapidity, and the midrapidity region remains unpopulated. Inclusion of the Coulomb field effect of the heavy partner on the fragmenting nucleus results in the forward-backward asymmetry in the emission pattern with respect to the source velocity. The Coulomb field pushes the heaviest fragments more apart leaving some more space for the lighter ones in between. Therefore the midrapidity region can be predominantly occupied by the light IMFs. Assuming the elliptical flow pattern, and thus deforming the sources even more, the midrapidity region can be filled completely (right column). Thus, by including the Coulomb field effect and adjusting the flow parameters it is possible, without losing the statistical equilibrium assumption, to produce asymmetry in the emission pattern, and account for at least a portion of midrapidity emissions in the framework of the statistical model.

3.2 Statistical and dynamical scenarios

An obvious candidate to describe the midrapidity emissions is of course a family of microscopic dynamical models (BUU [8], LV [9], Stochastic Meanfield [10], QMD [11], QPD [12], AMD [13], FMD [14]) which allow to study the temporal evolution of the system and incorporate the main ingredients of the nucleon-nucleon interactions. It has already been shown (see e.g. [15], [2], [3]), that some of them provide quite reasonable results as far as midrapidity emissions are concerned. Here we choose the molecular dynamics code CHIMERA [16] with the statistical sequential decay code GEMINI [17] used as an after-

burner, as a representative for a comparison with the experimental data.

Fig. 6 presents the results of such a comparison. The SMM predictions (left panels) and the results of a hybrid, CHIMERA plus GEMINI (right panels) are compared with the experimentally measured (middle panels) invariant cross sections of lithium ions emitted in peripheral Au+Au reaction at 80 MeV/nucleon.

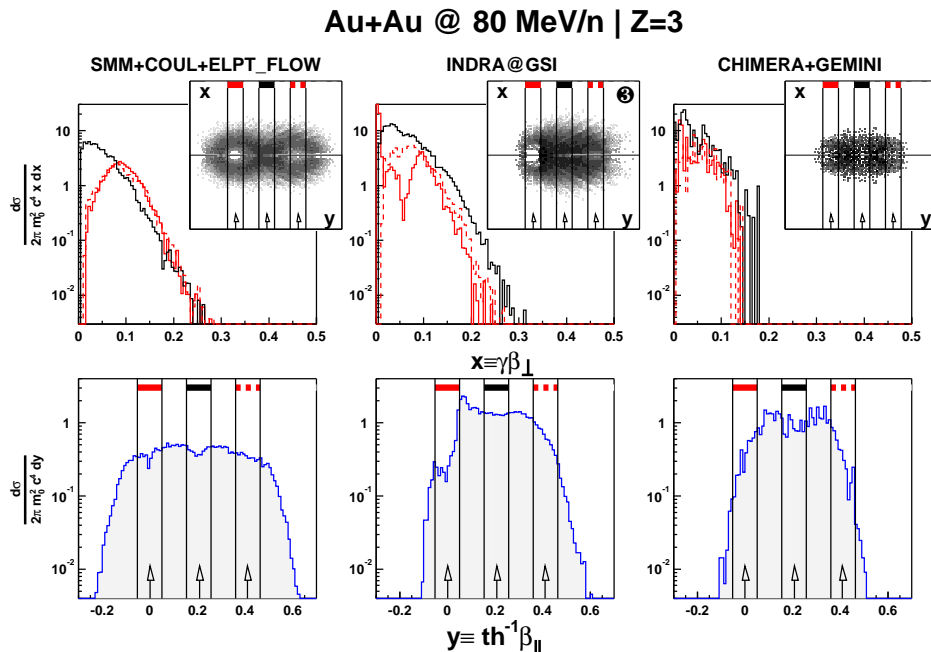


Figure 6: Invariant cross sections of lithium fragments emitted in peripheral reactions of Au+Au @ 80 MeV/n (insets) and their slices along the target, CM and projectile rapidities (upper row) and projections on rapidity axis (lower row). Left column: SMM prediction with the inclusion of Coulomb effect and elliptical flow (same as Fig. 5, right column); central column: experimental results for bin 3; right column: CHIMERA+GEMINI prediction for impact parameters 6-10 fm.

The above figure shows that, at least qualitatively, both models: statistical and dynamical, can account for midrapidity emissions. The remaining open question is how much of them originate from a statistically equilibrated source.

4 Transverse velocities and flow

The experimental transverse velocity spectra of fragments taken along the slices indicated in Figs. 5 and 6 by vertical lines (slices at midrapidity and at projectile rapidity) also show some interesting features.

Fig. 7 shows the experimental transverse velocity spectra of lithiums emitted in Au+Au reactions at various energies. The spectra were measured at midrapidity. An interesting observation can be drawn from this figure. At 40 MeV/nucleon and also perhaps at 50, the spectra have similar shapes independently of the centrality of the collision, from peripheral to central. Some dependence on the centrality starts at 60 MeV/nucleon incident energy. This qualitative observation can probably be attributed to the onset of flow, which starts to be of importance around that energy (see [18], [19]).

On the other hand, transverse velocity spectra taken at projectile rapidity for peripheral collisions, do almost not depend on the incident energy in a broad range from 40 to

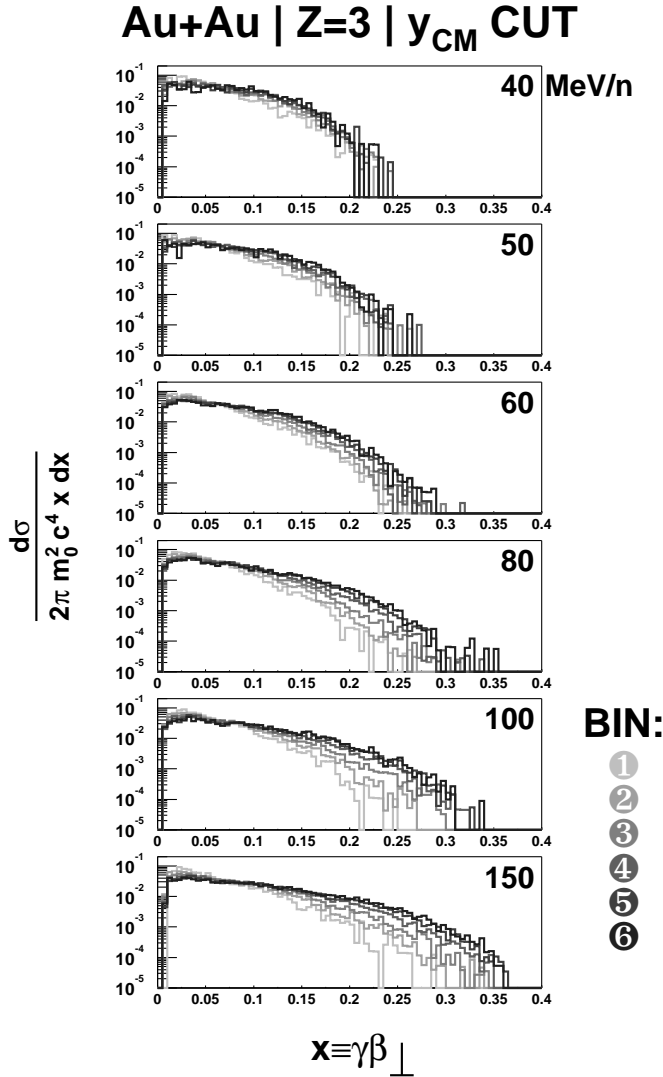


Figure 7: Transverse velocity spectra of lithium fragments emitted at midrapidity in the reaction of Au+Au for different centrality bins and incident energies from 40 to 150 MeV/nucleon.

150 MeV/nucleon. The observation seems to be consistent with the one for Xe+Sn from 25 to 50 MeV/nucleon [3]. Does it imply independence of the excitation energy per nucleon of the incident energy for a given impact parameter? This requires a further study.

5 Summary and outlook

The presented analysis was performed as a function of incident energy and of impact parameter, defined through the total transverse energy of light charged particles ($E_{trans12}$). This observable was found to be a suitable measure of centrality of the collision for both symmetric and asymmetric systems. For a given system, $E_{trans12}$ was found to scale linearly with the available energy up to certain limit of available energy. Deviations from linear scaling above this limit were partly attributed to the anisotropy of the nucleon - nucleon cross section.

It was shown that it is possible to attribute the origin of at least a fraction of midrapidity emissions to the thermal source. The presented analysis remains still on a qualitative level. Clear separation of the equilibrated and the dynamical components requires further studies, including a consistent statistical treatment and a careful adjustment of flow, and possibly inclusion of angular momentum and deformation effects in statistical mod-

els. Dynamical models in turn should be traced more carefully in terms of emission and equilibration times.

Direct inspection of transverse velocity spectra at midrapidity seems to confirm the onset of flow around 50-60 MeV/nucleon.

References

- [1] J.F. Dempsey *et al.* Phys. Rev. C **54**, 1710 (1996).
- [2] J. Lukasik *et al.* Phys. Rev. C **55**, 1906 (1997).
- [3] E. Plagnol *et al.* Phys. Rev. C **61**, 014606 (2000).
- [4] J. Pouthas *et al.*, Nucl. Instr. Meth. in Phys. Res. **A357** (1995) 418.
- [5] C. Cavata *et al.*, Phys. Rev. **C42** (1990) 1760.
- [6] J.P. Bondorf *et al.* Phys. Rep. **257**, 133 (1995),
A.S. Botvina *et al.* GSI Preprint 2000-50.
- [7] A.S. Botvina *et al.* Phys. Rev. **C59** (1999) 3444.
- [8] G.F. Bertsch, H. Kruse and S. Das Gupta, Phys. Rev. C **29** (1984) 673
J. Aichelin and G.F. Bertsch, Phys. Rev. C **31** (1985) 1730
- [9] J. Cugnon, A. Lejeune and P. Grangé, Phys. Rev. C **35** (1987) 861R
- [10] M. Colonna and Ph. Chomaz, Phys. Rev. C **49** (1994) 1908
- [11] J. Aichelin and H. Stöcker, Phys. Lett. **176B** (1986) 14
- [12] D.H. Boal and J.N. Glosli, Phys. Rev. C **38** (1988) 2621
- [13] A. Ono, H. Horiuchi, T. Maruyama and A. Ohnishi, Phys. Rev. Lett. **68** (1992) 2898
- [14] H. Feldmeier, Nucl. Phys. **A515** (1990) 147
- [15] Ph. Eudes *et al.*, Phys. Rev. C **56**, 2003 (1997).
- [16] J. Lukasik and Z. Majka Acta Phys. Pol. B **24**, 1959 (1993).
- [17] R.J. Charity *et al.*, Nuc. Phys. **A483** (1988) 371, **A511** (1988) 59
- [18] W. Reisdorf and H.G. Ritter, Annu. Rev. Nucl. Part. Sci. **47**, 663 (1997).
- [19] F. Lavaud *et al.*, see these proceedings.